

Efficient Approach to Time-Dependent Density-Functional Perturbation Theory for Optical Spectroscopy

Brent Walker,^{1,2} A. Marco Saitta,³ Ralph Gebauer,^{1,2} and Stefano Baroni^{4,2}

¹*ICTP—The Abdus Salam International Centre for Theoretical Physics, Strada Costiera 11, I-34014 Trieste, Italy*

²*DEMOCRITOS National Simulation Center, CNR-INFN, Trieste, Italy*

³*Institut de Minéralogie et de Physique des Milieux Condensés, Université Pierre et Marie Curie, Paris, France*

⁴*SISSA—Scuola Internazionale Superiore di Studi Avanzati, Via Beirut 2-4, I-34014 Trieste, Italy*

(Received 17 August 2005; published 20 March 2006)

Using a superoperator formulation of linearized time-dependent density-functional theory, the dynamical polarizability of a system of interacting electrons is represented by a matrix continued fraction whose coefficients can be obtained from the nonsymmetric block-Lanczos method. The resulting algorithm, which is particularly convenient when large basis sets are used, allows for the calculation of the *full spectrum* of a system with a computational workload only a few times larger than needed for *static* polarizabilities within time-independent density-functional perturbation theory. The method is demonstrated with calculation of the spectrum of benzene, and prospects for its application to the large-scale calculation of optical spectra are discussed.

DOI: [10.1103/PhysRevLett.96.113001](https://doi.org/10.1103/PhysRevLett.96.113001)

PACS numbers: 31.15.Ew, 33.20.Lg, 71.15.Mb, 71.15.Qe

The past two decades have witnessed the tremendous success of density-functional theory (DFT) [1] in describing and predicting various properties of systems of interacting electrons, from atoms and molecules to solids and liquids. In its original formulation, DFT only applies to the electronic ground state. This limitation was lifted by Runge and Gross (RG) [2] who generalized DFT to time-dependent (TD) systems. According to the RG theorem, for any given initial state of a many-electron system, the TD potential acting on it is uniquely determined by the subsequent time evolution of the one-electron density. Using this theorem, it is possible to formally establish a TD Kohn-Sham (KS) equation from which various one-particle properties of the system can be obtained as functions of time. The resulting theoretical framework is usually referred to as time-dependent density-functional theory (TDDFT). Most existing applications of TDDFT are based on the *adiabatic* exchange-correlation (XC) approximation (AXCA), which amounts to using the same functional dependence of the XC potential upon density as in the static case. Despite the crudeness of this approximation, optical spectra calculated from it are in some cases almost as accurate as those from more computationally demanding approaches based on many-body perturbation theory (MBPT) [3].

By linearizing the KS equations with respect to a time-dependent perturbation, TDDFT can be formulated in terms of a Dyson equation for the system's response functions. This approach allows for a straightforward conceptual juxtaposition of TDDFT and MBPT [3], as well as for a deep insight into the nature of the TDDFT XC kernel [4]. Computationally much lighter than MBPT, this approach still requires the manipulation (inversion, multiplication) of large matrices, which is hard to accomplish for large systems or basis sets. Also, many unoccupied eigenstates of the unperturbed KS Hamiltonian need to be calculated, a

task which again may become critical for large systems or basis sets, as it is easily the case with plane waves (PW's) or real-space grids. The poles of the response functions and their residues are excitation energies and oscillator strengths, respectively. The latter can also be obtained from the eigenvalues and eigenvectors of an appropriate non-Hermitian eigenvalue problem [5]. This problem has the same structure as in the TD Hartree-Fock theory [6], and the dimension of the resulting matrix (the *Liouvillian*) is twice the product of the number of occupied states with the number of unoccupied states. The calculation of a few eigenstates of such a large matrix can be accomplished using iterative techniques [7], possibly in conjunction with the Tamm-Dancoff approximation (TDA), which amounts to enforcing Hermiticity by neglecting the anti-Hermitian component of the Liouvillian [8]. Many existing molecular applications of TDDFT have been performed within such a framework which is probably near to optimal when a small number of excited states is required. In a large system, however, the number of quantum states in any given energy range grows with the system size. The number of pseudo-discrete states in the continuum grows with the basis-set size even in a small system. For these reasons, a method to model the absorption spectrum directly, without calculating individual excited states, would thus be highly desirable. Yabana and Bertsch proposed such an alternative approach where the TD-KS equations are solved in the time domain, and susceptibilities obtained by Fourier analyzing the linear response of the system to appropriate perturbations [9]. This scheme has the same numerical complexity as ground-state DFT iterative methods, and it also gives easy access to nonlinear optical properties. Because of this, real-time methods have recently gained popularity in conjunction with the use of real-space grids [10]. The main limitation is here that stable integration of the TD-KS equations requires a time step as small as

$\sim 10^{-3}$ fs in typical pseudopotential (PP) applications, which decreases as the number of grid points or PW's increases.

In this Letter we propose a novel way to calculate optical spectra in the frequency domain—thus avoiding any explicit integration of the TD-KS equations—which does not require the calculation of any unoccupied KS states, any time-consuming matrix operations, nor the calculation of individual eigenstates of the TDDFT Liouvillian. We express a generalized susceptibility as an off-diagonal matrix element of the resolvent of the Liouvillian superoperator, which is evaluated using a Lanczos continued fraction technique. The resulting numerical complexity is of the same order as that of time-independent density-functional perturbation theory [11].

Our formalism starts from Casida's linear-response formulation of TDDFT [5]. A system, characterized in its ground state by the KS Hamiltonian \hat{H}_{KS}^0 , orbitals $\varphi_v^0(\mathbf{r})$, and orbital energies ϵ_v , is subject to an external perturbation whose Fourier transform is $\lambda(\omega)\tilde{V}'_{\text{ext}}(\mathbf{r}, \omega)$, where $\lambda(\omega)$ conventionally indicates its strength. The solutions of the TD-KS equation corresponding to the initial conditions $\varphi_v(\mathbf{r}, 0) = \varphi_v^0(\mathbf{r})$ are indicated by $\varphi_v(\mathbf{r}, t)$, and the corresponding response orbitals by $\varphi'_v(\mathbf{r}, t) = [e^{i\epsilon_v t}\varphi_v(\mathbf{r}, t) - \varphi_v^0(\mathbf{r})]$, with Fourier transforms: $\varphi'_v^+(\mathbf{r}) = \tilde{\varphi}'_v(\mathbf{r}, \omega)$, and $\varphi'_v^-(\mathbf{r}) = \tilde{\varphi}'_v^*(\mathbf{r}, -\omega)$. The φ_v^\pm orbitals can be chosen to be orthogonal to the KS occupied manifold. If we define $x_v(\mathbf{r}) = \frac{1}{2}[\varphi'_v^+(\mathbf{r}) + \varphi'_v^-(\mathbf{r})]$ and $y_v(\mathbf{r}) = \frac{1}{2}[\varphi'_v^+(\mathbf{r}) - \varphi'_v^-(\mathbf{r})]$, then the linearized equation of motion can be written in the form [5]:

$$(\omega - \mathcal{L})|\mathbf{x}, \mathbf{y}\rangle = |0, \mathbf{v}\rangle, \quad (1)$$

where the ket indicates a *supervector* consisting of an ordered pair of *batches* of orbitals, $\mathbf{x} = \{x_v(\mathbf{r})\}$ and $\mathbf{y} = \{y_v(\mathbf{r})\}$, and the batch \mathbf{v} is defined as $\mathbf{v} = \{\hat{P}_c \tilde{V}'_{\text{ext}}(\mathbf{r}, \omega)\varphi_v^0(\mathbf{r})\}$, \hat{P}_c being the projector onto the KS unoccupied manifold. The Liouvillian *superoperator* \mathcal{L} is defined as $\mathcal{L}|\mathbf{x}, \mathbf{y}\rangle = |\mathcal{D} \cdot \mathbf{y}, (\mathcal{D} + \mathcal{K}) \cdot \mathbf{x}\rangle$, where \mathcal{D} and \mathcal{K} are Hermitian operators acting on batches of orbitals, $\mathbf{u} = \{u_v(\mathbf{r})\}$, as $\mathcal{D} \cdot \mathbf{u} = \{(\hat{H}_{\text{KS}}^0 - \epsilon_v)u_v(\mathbf{r})\}$ and $\mathcal{K} \cdot \mathbf{u} = \{\varphi_v^0(\mathbf{r}) \sum_{v'} \int \kappa(\mathbf{r}, \mathbf{r}') \varphi_{v'}^0(\mathbf{r}') u_{v'}(\mathbf{r}') d\mathbf{r}'\}$, $\kappa(\mathbf{r}, \mathbf{r}')$ being the Hartree plus XC kernel. Equation (1) gives the response of the system to the external perturbation as a function of frequency. When $V'_{\text{ext}} = 0$, this equation reduces to a (non-Hermitian) eigenvalue problem whose normal modes describe the free oscillations of the system corresponding to electronic excitations [5].

In practice, one is seldom interested in the response of the system to the most general perturbation, or in individual excitation energies, but just in the frequency-dependent response of some *specific* property to some *specific* perturbation. Let us consider an observable, \hat{A} , whose TD linear response is given by $A(t) = 2 \text{Re} \sum_v \langle \varphi_v^0 | \hat{A} | \varphi'_v(t) \rangle$. Assuming that \hat{A} is time-reversal invariant, the Fourier transform of $A(t)$ is $\hat{A}(\omega) = \sum_v (\langle \varphi_v^0 | \hat{A} | \varphi_v^+ \rangle + \langle \varphi_v^0 | \hat{A} | \varphi_v^- \rangle) \equiv$

$2\lambda(\omega)\langle \mathbf{a}, 0 | \mathbf{x}, \mathbf{y} \rangle$, where $\mathbf{a} = \{\hat{A}\varphi_v^0\}$. A generalized susceptibility, $\chi_{\text{AV}}(\omega)$, can be defined $\hat{A}(\omega)/\lambda(\omega)$:

$$\chi_{\text{AV}}(\omega) = 2\langle \mathbf{a}, 0 | (\omega - \mathcal{L})^{-1} | 0, \mathbf{v} \rangle. \quad (2)$$

Equation (2) states that within TDDFT any susceptibility can be expressed as an appropriate *off-diagonal* matrix element of the resolvent of the Liouvillian superoperator. We now show how such a matrix element can be conveniently calculated using the non-Hermitian block-Lanczos algorithm (NHBLA) [12].

We define a *block*, $|\mathbf{Q}\rangle$, as a pair of orthogonal supervectors: $|\mathbf{Q}\rangle = \{ |Q_1\rangle, |Q_2\rangle \}$. The scalar product between two blocks, $\mathbf{s} = \langle \mathbf{P} | \mathbf{Q} \rangle$ is defined as the 2×2 matrix: $s_{ij} = \langle P_i | Q_j \rangle$, and the action of a superoperator on a block is defined as the block whose elements are the result of the action of the superoperator on each supervector of the original block: $\mathcal{L}\{ |Q_1\rangle, |Q_2\rangle \} \equiv \{ | \mathcal{L}Q_1 \rangle, | \mathcal{L}Q_2 \rangle \}$. Given two starting blocks, $|\mathbf{Q}^1\rangle$ and $|\mathbf{P}^1\rangle$ such that $\langle P_i^1 | Q_j^1 \rangle = \delta_{ij}$, the NHBLA generates a sequence of block pairs, $\{ |\mathbf{Q}^n\rangle, |\mathbf{P}^n\rangle \}$, such that: $\langle P_i^n | Q_j^m \rangle = \delta_{mn} \delta_{ij}$, and $\mathcal{L} = \sum_{nm, ij} T_{ij}^{nm} |Q_i^m\rangle \langle P_j^n|$, where $T_{ij}^{nm} = \langle P_i^n | \mathcal{L} | Q_j^m \rangle = a_{ij}^n \delta_{mn} + b_{ij}^n \delta_{m+1, n} + c_{ij}^m \delta_{m, n+1}$ is a block-tridiagonal matrix. The matrix element of the resolvent of the Liouvillian between the two elements of the starting block can then be easily expressed as a matrix continued fraction:

$$\langle \mathbf{P}_1 | (\omega - \mathcal{L})^{-1} | \mathbf{Q}_1 \rangle = \frac{1}{\omega - \mathbf{a}_1 + \mathbf{b}_2 \frac{1}{\omega - \mathbf{a}_2 + \dots} \mathbf{c}_2}, \quad (3)$$

where the \mathbf{a} 's, \mathbf{b} 's, and \mathbf{c} 's are 2×2 matrices. If the starting blocks are chosen as $|\mathbf{P}_1\rangle = |\mathbf{Q}_1\rangle = \{ |\mathbf{a}, 0\rangle, |0, \mathbf{v}\rangle \}$, the generalized susceptibility, Eq. (2), is then the (1,2) matrix element of the 2×2 matrix in Eq. (3). Without going into the details of the NHBLA, suffice it to say that its implementation does not require the explicit calculation of the Liouvillian superoperator, nor even of the unperturbed KS Hamiltonian, but just the availability of a black-box computer routine which, for any given batch of orbitals, $\mathbf{u} = \{u_v(\mathbf{r})\}$, returns $\mathcal{D}|\mathbf{u}\rangle$ and $\mathcal{K}|\mathbf{u}\rangle$. Each step of the NHBLA essentially involves two calls to such a routine, whose computational cost is roughly that of a single iteration in a static DFPT calculation. If the XC kernel is frequency independent, as is the case in the AXCA, the block-tridiagonal representation of \mathcal{L} is independent of frequency, and one single Lanczos chain allows for the calculation of the spectrum at all frequencies via Eq. (3). When the frequency dependence of the XC kernel is explicitly accounted for, the situation is not as simple, but it is possible that linearization of the kernel within selected frequency windows will result in a manageable scheme based on a single Lanczos chain per window. We finally notice that this method would also apply in the presence of nonlocal kernels—such as those occurring with hybrid functionals—once the action of the exchange operator

onto a molecular orbital is properly implemented for ground-state calculations.

To demonstrate our methodology, we calculate the absorption spectrum of benzene, a system for which many excited-state calculations already exist [13,14], some of which were performed within TDDFT [14]. Computational details are given in Ref. [15]. The convergence properties of our algorithm are displayed in Fig. 1, which reports the absorption spectrum of benzene for light polarized in the xy plane. We see that 2000–3000 steps are sufficient to ensure convergence for energies up to ≈ 15 eV. A direct comparison of the efficiency of approaches aimed at calculating individual eigenstates is basically impossible, whereas such a comparison is more meaningful with time-propagation methods. Our most well-converged spectrum is compared in the inset with that obtained from real-time propagation. The agreement is practically perfect. The number of time steps required to calculate the spectrum reported in the inset is 12 700, which is typical of this type of calculation. Each time step requires several Hamiltonian-wavefunction ($H\psi$) products, depending on the propagation scheme used [16]. In the present approach, each Lanczos step requires two $H\psi$ multiplications. Obtaining a converged spectrum is therefore numerically considerably less demanding than using a real-time propagation. Although a thorough theoretical analysis of the convergence properties of our algorithm is beyond the scope of this Letter, we point out a few facts that we believe will deserve further attention. Firstly the convergence properties deteriorate—not unexpectedly—with increasing frequency: the lower the frequency, the better the convergence. Secondly, the convergence rate of the algorithm is somewhat affected by the condition number of the Liouvillian, which depends on the size of the PW basis set: the higher the PW kinetic-energy cutoff, the poorer the convergence [17]. Furthermore, the numerical instabilities which are known to plague Lanczos diagonalization algo-

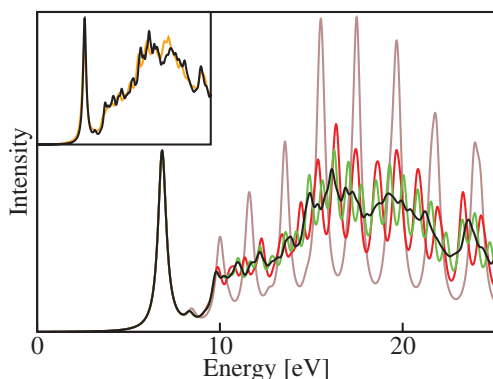


FIG. 1 (color). Absorption spectrum of benzene calculated using the Lanczos method with different numbers of recursion steps: 1000 (plum), 2000 (red), 3000 (green), and 6000 (black). The inset compares the 6000-step spectrum (black) with that obtained using the real-time propagation method (orange).

rithms [12] seem to have little, if any, effect on the calculation of the resolvent matrix elements through Eq. (3). As far as we can say, Eq. (3) can be pushed as far as needed to reach any desired level of accuracy. Finally, the non-Hermitian character of the Liouvillian reduces the efficiency of the algorithm, as can be seen from the performance of the TDA that we examine now. In Fig. 2 we compare the experimental absorption spectrum [18] with those obtained with our TDDFT method, with and without the TDA. Use of the TDA does not change much the overall appearance of the spectrum. The main differences are seen in the intensities and in a slight blue shift of the peaks that, when using the TDA, would therefore enhance a similar effect due to the inability of most of the current energy functionals to properly account for the electron-hole attraction. The convergence of TDA calculations is much faster than when using the full non-Hermitian form of the Liouvillian (see the inset of Fig. 2).

The agreement between the calculated and experimental spectra is very good, as known from previous TDDFT calculations for benzene [14]. The quality of this agreement is to some extent due to the nature of the molecular orbitals involved in the transitions dominating the low-lying part of the spectrum (π , π^* , and to a lesser extent, σ), which are little affected by the incorrect asymptotic behavior of the local-density AXCA potential. The absorption spectra shown in Fig. 2, though resulting from an average over different polarizations, are dominated by the $(\pi^* \leftarrow \pi)^1 E_{1u}$ transition which is only allowed when the light is polarized in the plane of the molecule. This transition is mainly responsible for the first strong absorption peak found experimentally at 6.94 eV, and predicted by TDDFT at 6.83 eV. Interestingly, the z component of the spectrum displays a weak peak at 6.55 eV, which is not visible in Fig. 2 (its intensity being less than one tenth that of the xy peak), corresponding to a $(\pi^* \leftarrow \sigma)^1 A_{2u}$ transi-

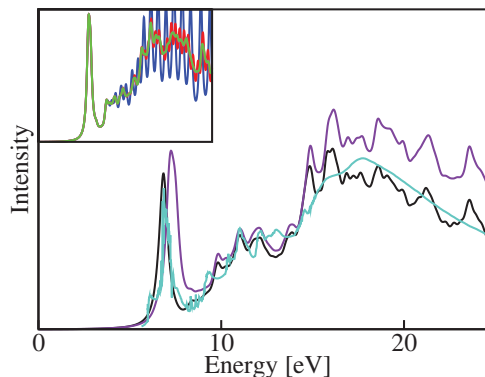


FIG. 2 (color). Comparison between the converged Lanczos spectrum obtained with the full non-Hermitian Liouvillian (black), the Tamm-Dancoff approximation (purple), and the experimental results (cyan). The inset shows the convergence of the TDA spectrum with respect to the number of recursion steps: 250 (blue), 500 (red), 1000 (magenta), and 2000 (green).

tion. In the independent-electron approximation, this transition would have a higher energy than ${}^1E_{1u}$, which corresponds to the highest-occupied-molecular-orbital–lowest-unoccupied-molecular-orbital gap. The red shift of the ${}^1A_{2u}$ transition is therefore due to the effects of the electron-electron interaction which are approximately accounted for in AXCA-TDDFT. The ${}^1A_{2u}$ transition has never been detected directly in absorption experiments, but its existence (as well as its location near, possibly at a lower frequency than, the strong ${}^1E_{1u}$ transition) was inferred from Raman scattering experiments [19]. The proximity of the ${}^1E_{1u}$ and ${}^1A_{2u}$, and the much lower intensity of the latter, were also confirmed by accurate coupled-cluster calculations [13(d)]. It is possible that the little shoulder observed at 6.19 eV in the absorption spectrum [18] and attributed to a vibron-assisted ${}^1B_{1u}$ forbidden excitation, is actually due to a weak ${}^1A_{2u}$ allowed transition.

We believe that the method presented in this Letter, while not touching on our serious ignorance on the form of TD XC functionals, will open the way to the study of systems which are too large to be treated at present. The scaling with system or basis-set size of a single iteration is basically the same as in ground-state methods, such as energy minimization or *ab initio* molecular dynamics. The size dependence of the number of required iterations is an issue which will only be settled by extensive experimentation. These already rather favorable numerical features will be further improved by the use of ultrasoft PP's (allowing for the reduction of both the size of one-electron basis sets and the condition number of the Liouvillian), and by devising optimal strategies for restarting the Lanczos chain using approximate schemes. Work is in progress along these lines.

S. B. thanks Y. Saad for useful discussions, and A. Polian and R. Wentzcovitch for hospitality at the University of Paris VI, where this work was started, and at the University of Minnesota *vLab*, where most of this Letter was written.

[1] P. Hohenberg and W. Kohn, Phys. Rev. **136**, B864 (1964); W. Kohn and L. J. Sham, Phys. Rev. **140**, A1133 (1965).
 [2] E. Runge and E. K. U. Gross, Phys. Rev. Lett. **52**, 997 (1984).
 [3] G. Onida, L. Reining, and A. Rubio, Rev. Mod. Phys. **74**, 601 (2002).
 [4] L. Reining, V. Olevano, A. Rubio, and G. Onida, Phys. Rev. Lett. **88**, 066404 (2002).
 [5] M. E. Casida, in *Recent Advances in Density Functional Methods Part I*, edited by D. P. Chong (World Scientific, Singapore, 1995), p. 155; M. E. Casida, J. Chem. Phys. **122**, 054111 (2005).
 [6] See, e.g., A. D. McLachlan and M. A. Ball, Rev. Mod. Phys. **36**, 844 (1964).
 [7] R. E. Stratmann, G. E. Scuseria, and M. J. Frisch, J. Chem. Phys. **109**, 8218 (1998).

[8] I. Tamm, J. Phys. (Moscow) **9**, 449 (1945); S. M. Dancoff, Phys. Rev. **78**, 382 (1950); S. Hirata and M. Head-Gordon, Chem. Phys. Lett. **314**, 291 (1999).
 [9] K. Yabana and G. F. Bertsch, Phys. Rev. B **54**, 4484 (1996).
 [10] G. F. Bertsch, J.-I. Iwata, A. Rubio, and K. Yabana, Phys. Rev. B **62**, 7998 (2000); M. A. L. Marques, X. Lopez, D. Varsano, A. Castro, and A. Rubio, Phys. Rev. Lett. **90**, 258101 (2003).
 [11] (a) S. Baroni, P. Giannozzi, and A. Testa, Phys. Rev. Lett. **58**, 1861 (1987); (b) S. Baroni, S. de Gironcoli, A. Dal Corso, and P. Giannozzi, Rev. Mod. Phys. **73**, 515 (2001).
 [12] Z. Bai and D. Day, *Templates for the Solution of Algebraic Eigenvalue Problems: A Practical Guide*, Block Lanczos Methods (Section 7.9), edited by Z. Bai, J. Demmel, J. Dongarra, A. Ruhe, and H. van der Vorst (SIAM, Philadelphia, 2000).
 [13] (a) J. Lorentzon, P.-A. Malmquist, M. Fulscher, and B. O. Roos, Theor. Chim. Acta **91**, 91 (1995); (b) M. J. Packer, E. K. Dalskov, T. Enevoldsen, H. J. Jensen, and J. J. Oddershede, J. Chem. Phys. **105**, 5886 (1996); (c) O. Christiansen, H. Koch, A. Halkier, P. Jørgensen, T. Helgaker, and A. S. de Meras, J. Chem. Phys. **105**, 6921 (1996); (d) A. Christiansen, C. Hättig, and P. Jørgensen, Spectrochim. Acta, Part A **55**, 509 (1999).
 [14] N. C. Handy and D. J. Tozer, J. Comput. Chem. **20**, 106 (1999); K. Yabana and G. F. Bertsch, Int. J. Quantum Chem. **75**, 55 (1999); H. H. Heinze, A. Görling, and N. Rösch, J. Chem. Phys. **113**, 2088 (2000).
 [15] Our method was implemented on top of the PWSCF PW PP code, part of the *Quantum ESPRESSO* distribution (see <http://www.quantum-espresso.org/> and <http://www.pwscf.org/>). The KS equations for an isolated benzene molecule were solved using periodic boundary conditions (PBC's) in a tetragonal simulation cell with its base, parallel to the carbon ring ("xy" plane), of side length 30.0 Å, and with height 2/3 of this; the CC and CH bond lengths were 1.40 Å and 1.09 Å, respectively. A simple local density approximation XC functional was adopted [J. P. Perdew and A. Zunger, Phys. Rev. B **23**, 5048 (1981)]. Norm-conserving PP's "C.pz-vbc.UPF" and "H.pz-vbc.UPF" from the PWscf table (<http://www.pwscf.org/pseudo.htm>) were used for carbon and hydrogen, respectively. A PW kinetic-energy cutoff of 60.0 Ry, corresponding to 70 600 PW's, was adopted. The resulting dimension of the Liouvillian superoperator exceeds 1 000 000. The PBC calculation of dipole matrix elements was performed as explained in Sec. C.2 of Ref. [11(b)]. The absorption coefficient was obtained as $I(\omega) \propto \omega \text{Im}\chi(\omega)$ is the electric dipole susceptibility, Eq. (2), calculated at complex frequencies with an imaginary part of 0.27 eV.
 [16] A. Castro, M. A. L. Marques, and A. Rubio, J. Chem. Phys. **121**, 3425 (2004).
 [17] For silane the spectrum, calculated with a kinetic-energy cutoff of 35 Ry, shows full convergence with a number of Lanczos recursions between 1000 and 2000.
 [18] E. E. Koch and A. Otto, Chem. Phys. Lett. **12**, 476 (1972).
 [19] L. Ziegler and A. C. Albrecht, J. Chem. Phys. **67**, 2753 (1977); M. Ito, H. Abe, and J. Murakami, J. Chem. Phys. **69**, 606 (1978).